arXiv:cond-mat/0309601v1 [cond-mat.stat-mech] 26 Sep 2003

Stabilization of the number of Bose-Einstein condensed atoms in evaporative cooling via three-body recombination loss

Makoto Yamashita and Tetsuya Mukai
NTT Basic Research Laboratories, NTT Corporation, 3-1,
Morinosato-Wakamiya, Atsugi-shi, Kanagawa 243-0198, Japan

The dynamics of evaporative cooling of magnetically trapped ^{87}Rb atoms is studied on the basis of the quantum kinetic theory of a Bose gas. We carried out the quantitative calculations of the time evolution of conventional evaporative cooling where the frequency of the radio-frequency magnetic field is swept exponentially. This "exponential-sweep cooling" is known to become inefficient at the final stage of the cooling process due to a serious three-body recombination loss. We precisely examine how the growth of a Bose-Einstein condensate depends on the experimental parameters of evaporative cooling, such as the initial number of trapped atoms, the initial temperature, and the bias field of a magnetic trap. It is shown that three-body recombination drastically depletes the trapped ^{87}Rb atoms as the system approaches the quantum degenerate region and the number of condensed atoms finally becomes insensitive to these experimental parameters. This result indicates that the final number of condensed atoms is well stabilized by a large nonlinear three-body loss against the fluctuations of experimental conditions in evaporative cooling.

I. INTRODUCTION

Evaporative cooling is the key experimental technique in recent successful demonstrations of Bose-Einstein condensation (BEC) with trapped neutral atoms [1, 2, 3, 4, 5]. The cooling mechanism is understood to be that evaporation caused by atomic collisions selectively removes the energetic atoms and collisional rethermalization simultaneously lowers the temperature of atoms remaining in a trap [6, 7]. The utilization of interatomic elastic collisions makes evaporative cooling highly efficient. Ultralow temperatures of the order of submicro-Kelvin have been achieved in BEC experiments by applying evaporative cooling to laser-cooled atoms. However, in the case of real atoms, other undesirable collisions occur, such as elastic collisions with background gas and inelastic collisions due to dipolar relaxation and three-body recombination [6, 7]. These collisions result in the loss of trapped atoms and seriously reduce the effectiveness of evaporative cooling. The efficiency of evaporative cooling is therefore determined by the competition between evaporation and the loss due to the undesirable collisions.

Several theoretical analyses based on a classical gas model have addressed the complicated dynamics of evaporative cooling [6, 7, 8, 9, 10, 11, 12, 13, 14, 15, 16, 17]. The results have been applied to the optimization of experimental conditions [15, 17] and have provided useful guidelines for reaching the BEC transition point experimentally. However, the classical theories fail in the quantum degenerate region at low temperatures. Bose statistics of atoms strongly modifies the dynamics of evaporative cooling there: interatomic elastic collisions are enhanced by the stimulated scattering process, and the event rates of inelastic collisions due to dipolar relaxation and three-body recombination are reduced by the coherence of identical condensed atoms [18, 19, 20]. Recent theoretical works [21, 22, 23, 24, 25, 26] have proved that the quantum kinetic theory taking into account the bosonic nature of atoms is a powerful tool to gain a comprehensive understanding of evaporative cooling in BEC experiments.

In our previous paper [27], we studied the optimization of evaporative cooling in a magnetically trapped ^{87}Rb system on the basis of the quantum kinetic theory. We demonstrated that the acceleration of evaporative cooling around the BEC transition point is very effective against the loss of trapped atoms due to three-body recombination. The number of condensed atoms is largely enhanced by simply optimizing a sweeping function of the frequency of radio-frequency (rf) magnetic field. On the other hand, this optimized cooling is determined for a fixed certain experimental condition and its cooling trajectory is sensitive to the experimental parameters of evaporative cooling, such as the initial number of trapped atoms and the initial temperature. The optimized evaporative cooling therefore might show the fluctuations of the final number of condensed atoms due to some variations of these experimental parameters inherent in the real experiments. In current BEC experiments, the number of condensed atoms is usually measured by the destructive time-of-flight method. The stable production of condensates with small number-fluctuations is thought to be another essential property of evaporative cooling.

In this paper, we quantitatively analyze the dynamics of the conventional evaporative cooling where rf-frequency is swept exponentially. This "exponential-sweep cooling" is known to become inefficient at the last stage of the cooling process due to three-body recombination loss. We precisely examine the dependence of condensate growth on the experimental parameters, such as the initial number of trapped atoms, the initial temperature, and the bias field of magnetic trap. We demonstrate that three-body loss drastically depletes the trapped ^{87}Rb atoms around the BEC transition point and that the number of condensed atoms finally becomes insensitive to these experimental parameters. The final number of condensed atoms is well stabilized by a large nonlinear three-body loss against the fluctuations of experimental conditions.

II. QUANTUM KINETIC THEORY OF EVAPORATIVE COOLING

In this section, we briefly mention our theoretical framework (See Ref. [24]). During evaporative cooling, the magnetic trapping potential $U(\mathbf{r})$ is truncated at the energy, which is determined by the frequency of the applied rf-magnetic field. The thermalized distribution of the noncondensed atoms in such a truncated potential is well described by the truncated Bose-Einstein distribution function such that

$$\tilde{f}(\mathbf{r},p) = \frac{1}{\exp(\epsilon_p/k_B T)/\tilde{\xi}(\mathbf{r}) - 1}\ \Theta(\tilde{A}(\mathbf{r}) - \epsilon_p), \qquad (1)$$

where $\epsilon_p = p^2/2m$ is the kinetic energy of atoms with momentum p and mass m, T is the temperature, and $\Theta(x)$ is the step function. We add tilde to the notations of the quantities obtained through this truncated distribution function. The function $\tilde{\xi}(\mathbf{r})$ represents the local fugacity and includes the mean-field potential energy such that $\xi(\mathbf{r}) = \exp\{[\mu - U(\mathbf{r}) - 2v\tilde{n}(\mathbf{r})]/k_B T\}$, where μ is the chemical potential, $v = 4\pi a\hbar^2$ the interaction strength of atoms in proportional to the s-wave scattering length a, and $\tilde{n}(\mathbf{r})$ the number density of atoms. The step function in Eq. (1) eliminates the momentum state whose kinetic energy exceeds the effective potential depth $\tilde{A}(\mathbf{r}) = \epsilon_t - U(\mathbf{r}) - 2v\tilde{n}(\mathbf{r})$, where ϵ_t is the truncation energy of a magnetic trapping potential. The number density of atoms $\tilde{n}(\mathbf{r})$ and the internal energy density $\tilde{e}(\mathbf{r})$ are evaluated through the truncated distribution function in a self-consistent way:

$$\begin{aligned} \tilde{n}(\mathbf{r}) &= \frac{4\pi}{h^3}\int \tilde{f}(\mathbf{r},p)\ p^2 dp, & (2) \\ \tilde{e}(\mathbf{r}) &= \frac{4\pi}{h^3}\int \epsilon_p\ \tilde{f}(\mathbf{r},p)\ p^2 dp + v[\tilde{n}(\mathbf{r})]^2 \\ &\quad + U(\mathbf{r})\tilde{n}(\mathbf{r}). & (3) \end{aligned}$$

Thus both $\tilde{n}(\mathbf{r})$ and $\tilde{e}(\mathbf{r})$ are the complicated functions of T, μ, ϵ_t, $U(\mathbf{r})$, and a. The spatial integrations of these density functions give us the total number of atoms, $\tilde{N} = \int \tilde{n}(\mathbf{r})d\mathbf{r}$, and the total internal energy, $\tilde{E} = \int \tilde{e}(\mathbf{r})d\mathbf{r}$. After the BEC transition, the number density in the condensed region is given by the sum of a condensate $n_0(\mathbf{r})$ and saturated noncondensed atoms $\tilde{n}_n$ such that $\tilde{n}(\mathbf{r}) = n_0(\mathbf{r}) + \tilde{n}_n$. The condensate $n_0(\mathbf{r})$ is approximated by the Thomas-Fermi distribution and $\tilde{n}_n$ is evaluated from the truncated Bose-Einstein distribution function on the condition that the local fugacity becomes unity, i.e., $\tilde{\xi}(\mathbf{r}) = 1$.

During the cooling process, trapped atoms are removed from the potential by both evaporation and undesirable collisions. The change rates of the total number of atoms, $\tilde{N}$, and the total internal energy, $\tilde{E}$, are thus calculated as the sum of the contributions of all processes [27]:

$$\begin{aligned} \frac{d\tilde{N}}{dt} &= -\int \dot{n}_{\rm ev}(\mathbf{r})\ d\mathbf{r} - \sum_{s=1}^{3} G_s \int K_s(\mathbf{r})[\tilde{n}(\mathbf{r})]^s\ d\mathbf{r} \\ &\quad + \left(\frac{\partial \tilde{N}}{\partial \epsilon_t}\right)_{T,\mu} \dot{\epsilon}_t, & (4) \\ \frac{d\tilde{E}}{dt} &= -\int \dot{e}_{\rm ev}(\mathbf{r})\ d\mathbf{r} - \sum_{s=1}^{3} G_s \int K_s(\mathbf{r})\tilde{e}(\mathbf{r})[\tilde{n}(\mathbf{r})]^{s-1}\ d\mathbf{r} \\ &\quad + \left(\frac{\partial \tilde{E}}{\partial \epsilon_t}\right)_{T,\mu} \dot{\epsilon}_t. & (5) \end{aligned}$$

The $\dot{n}_{\rm ev}(\mathbf{r})$ and $\dot{e}_{\rm ev}(\mathbf{r})$ denote the evaporation rates of density functions derived from a general collision integral of a Bose gas system. In Eqs. (4) and (5), we adopt the opposite sign of the notations of these evaporation rates, which were defined in our previous paper [24]. Parameters G_1, G_2, and G_3 are the decay rate constants of trapped atoms due to the background gas collisions, dipolar relaxation, and three-body recombination, respectively. The function $K_s(\mathbf{r})$ represents the correlation function, which describes the s-th order coherence of trapped atoms, and we use the expressions of K_s for an ideal Bose gas system [18, 19, 20]. The terms proportional to the change rate of truncation energy, $\dot{\epsilon}_t = d\epsilon_t/dt$, give the contribution of extra atoms that “spill over” when ϵ_t decreases continuously in forced evaporative cooling [16, 27].

The time-evolution was calculated numerically by assuming that the system always stays in quasi-thermal equilibrium state and is described by the truncated Bose-Einstein distribution function. This quick rethermalization approximation is appropriate for the slow evaporative cooling normally adopted in BEC experiments [13, 24].

III. NUMERICAL RESULTS AND DISCUSSINS

In this section, we show the numerical results of the time-evolution calculations of evaporative cooling corresponding to the several cases of experimental conditions. To carry out the quantitative calculations, we employed the relevant parameters corresponding to the experimental setup at Gakushuin University [28]. The cloverleaf magnetic trap characterized by bias field B_0, radial gradient $B^{'}$, and axial curvature $B^{''}$ was modeled by a magnetic field of the Ioffe-Pritchard type such that $B(r,z) = \sqrt{(\alpha r)^2 + (\beta z^2 + B_0)^2}$, where $\alpha = \sqrt{B'^2 - B''B_0/2}$ and $\beta = B^{''}/2$. We used the typical values adopted experimentally, such as $B_0 = 1.6$ G, $B^{'} = 169$ G/cm, and

$B'' = 148$ G/cm^2. The corresponding trapping frequencies are $\omega_r = 2\pi \times 170$ Hz in the radial direction and $\omega_z = 2\pi \times 15.5$ Hz in the axial direction.

The frequency of the rf-magnetic field, ν_{rf}, is assumed to be swept exponentially from 35 to 1.13 MHz in 30 s such that $\nu_{\mathrm{rf}}(t) = \nu_a + (\nu_b - \nu_a)\ e^{-t/\tau}$ with $\nu_a = 1.13$ MHz, $\nu_b = 35$ MHz, and $\tau = 3.69$ s. This exponential-sweep cooling is commonly adopted in BEC experiments [20], and we employed this functional form in the following all numerical calculations. Furthermore, we set the collisional parameters of ^{87}Rb atoms in the trapped state of $\mathrm{F} = 2, \mathrm{m_F} = +2$ as follows: s-wave scattering length $a = 5.8$ nm, loss rate constants due to collisions with background gas $G_1 = 0.01$ s^{-1}, dipolar relaxation $G_2 = 1.0 \times 10^{-15}$ cm^{3}s^{-1} [29], and three-body relaxation $G_3 = 1.1 \times 10^{-28}$ cm^{6}s^{-1} [20].

A. Dependence on the initial number of trapped atoms

Considering that the initial temperature is strongly restricted by the limit of the laser cooling done before evaporative cooling [30], we first carried out the time-evolution calculations for several initial numbers of atoms with the initial temperature fixed. Under the typical initial temperature of $T_i = 380$ μK [28], we varied the initial total number of atoms from $N_i = 1.5 \times 10^8$ to 3×10^9 and investigated how the final number of condensed atoms depends on these values.

Figures 1(a) and 1(b) respectively show the time-evolution of the total number of atoms $\tilde{N}$ and temperature T for several initial conditions of evaporative cooling. We can see that both $\tilde{N}$ and T decrease almost exponentially over time. Furthermore, in Fig. 1(a), four of the curves from the solid line to the dash-dotted line corresponding to $N_i = 3 \times 10^8 \sim 3 \times 10^9$ merge into one, which means ten times more initial atoms are completely lost during the 30-s cooling. The time-evolution of temperature in Fig. 1(b) also shows the same feature. The final results of exponential-sweep evaporative cooling become insensitive to the initial number of atoms when cooling starts from more than 3×10^8 atoms.

Figure 2 shows the dependence of the time evolution of the number of condensed atoms, N_0, on the initial number of trapped atoms N_i. For $N_i = 3 \times 10^8 \sim 3 \times 10^9$, we finally obtain the same N_0 value of 8.3×10^4 with the same condensate fraction of $N_0/\tilde{N} = 51\%$ after 30-s evaporative cooling, even though the BEC transition occurs at a different time. This implies that, when we apply exponential-sweep evaporative cooling, even a one-order change of the initial total number of trapped atoms does not affect the final number of condensed atoms. Since $N_i = (3 \sim 5) \times 10^8$ is normally achieved in current BEC experiments with ^{87}Rb, it is concluded that the final number of condensed atoms can be well stabilized against the fluctuations of the initial number of atoms in the experiments.

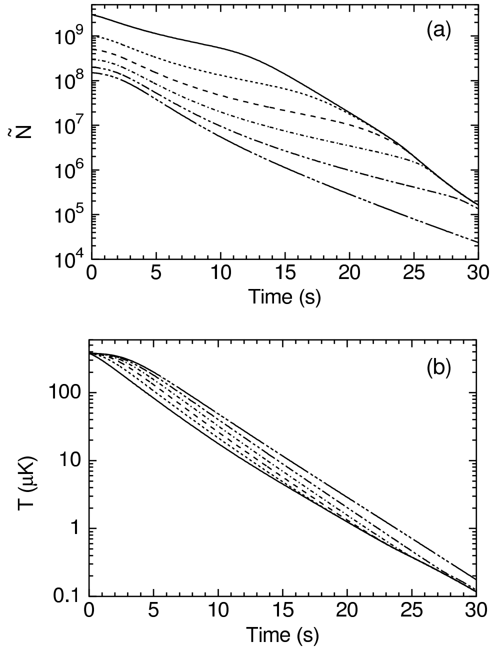

FIG. 1: Time evolution of (a) total number of atoms $\tilde{N}$ and (b) temperature T for several initial conditions of evaporative cooling: the initial number of trapped atoms N_i is varied from 1.5×10^8 to 3×10^9 under the fixed initial temperature of $T_i = 380$ μK. In both figures, the curves correspond to cases with $N_i = 1.5 \times 10^8$ (—‑‑‑‑—), 2×10^8 (—‑‑‑—), 3×10^8 (—·—), 5×10^8 (‑ ‑ ‑), 1×10^9 (·········), and 3×10^9 (———).

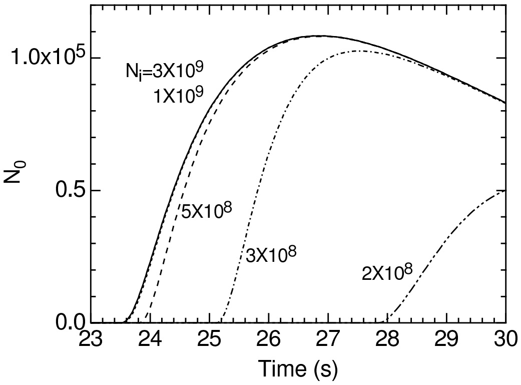

FIG. 2: Time evolution of the number of condensed atoms N_0 for the several initial numbers of trapped atoms N_i. We use the same lines as in Fig. 1 in terms of the corresponding N_i values. The solid line ($N_i = 3 \times 10^9$) and the dotted line ($N_i = 1 \times 10^9$) almost coincide with each other. For $N_i = 1.5 \times 10^8$, the system can not reach the BEC transition point and condensed atoms are not produced.

Here we show the results of the cooling trajectory through phase space and provide clear information about the efficiencies of present exponential-sweep cooling. In a nonuniform gas system, the phase-space density is evaluated at the peak position as $\tilde{\rho} = \tilde{n}(\mathbf{0})\lambda^3$, where $\lambda = h/\sqrt{2\pi m k_B T}$ is the thermal de Broglie wavelength with atomic mass m. In Fig. 3, we plot the cooling

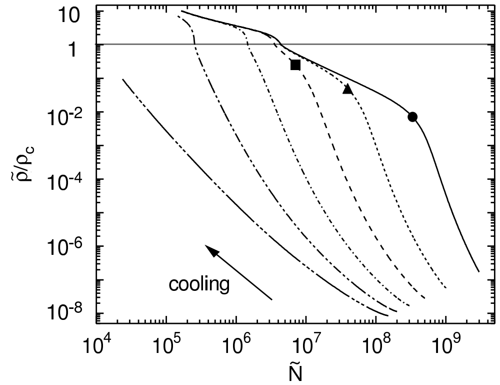

FIG. 3: Cooling trajectories through phase space for several initial conditions of evaporative cooling: the initial number of trapped atoms N_i is varied under the fixed initial temperature of $T_i = 380$ μK. The phase-space density $\tilde{\rho}$ is normalized by the critical value $\rho_c = 2.612$. The BEC transition occurs when each trajectory passes the horizontal line where $\tilde{\rho}/\rho_c = 1$. We use the same lines as in Fig. 1 in terms of the corresponding N_i values. The arrow shows the direction of time. The symbols on the solid line (circle), dotted line (triangle), and dashed line (square) indicate the points where the evaporative cooling becomes significantly inefficient.

trajectories of the present evaporative cooling in the $\tilde{N}$-$\tilde{\rho}$ plane. At the early stage of cooling, all trajectories are well separated according to the initial conditions and evaporative cooling works efficiently. However, as the system approaches the quantum degenerate region where the phase-space density exceeds the critical value of $\rho_c = 2.612$, three of the trajectories from the solid line to the dashed line bend towards horizontal around the respective turning points indicated by the symbols, showing the cooling efficiency drastically decreases there. As expected from the results in Fig. 1, three of the trajectories merge and finally coincide with the dash-dotted line corresponding to $N_i = 3 \times 10^8$. On the other hand, when $N_i \leq 2\times10^8$, the final results after 30-s evaporative cooling strongly depend on the initial number of atoms. The system can not reach the BEC transition point if the cooling is started from $N_i = 1.5 \times 10^8$.

Next, we show the loss rates of trapped atoms during evaporative cooling and discuss the origin of the inefficiency of cooling. As described in Eq. (4), the change rates of the total number of atoms decompose into five contributions: the evaporation rate $\dot{N}_{\rm ev}$, spill rate $\dot{N}_{\rm spill}$, loss rates due to back-ground gas collision $\dot{N}_1$, two-body dipolar relaxation $\dot{N}_2$, and three-body recombination $\dot{N}_3$. In Fig. 4, we plot the time evolution of these rates for $N_i = 3\times10^9, 1\times10^9$, and 5×10^8. The results for $\dot{N}_1$ are not shown here since this rate is given by $G_1\tilde{N}$ and evaluated straightforwardly from Fig. 1(a). The symbols in the figures correspond to the same points plotted on the cooling trajectories in Fig. 3 and indicate the time where the efficiency of evaporative cooling is drastically reduced. We see that both $\dot{N}_{\rm ev}$ and $\dot{N}_{\rm spill}$ [31] decrease exponentially over time, while $\dot{N}_2$ and $\dot{N}_3$ have peak structures around the symbol on each curve. The peak value of $\dot{N}_3$ is about five times larger than that of $\dot{N}_2$ and three-body recombination is the dominant loss mechanism for ^{87}Rb atoms. By comparing Fig. 4(a) with 4(d), it is also found that the symbol on each curve indicates the time when the three-body loss rate exceeds the evaporation rate. At the final stage of the present exponential-sweep cooling, we understand that the cooling speed becomes so low that the three-body loss crucially reduces the cooling efficiency. A stabilization of the final number of condensed atoms is therefore realized by the combination of slow cooling and large three-body loss.

From another viewpoint, the present result also suggests that the exponential-sweep of rf-frequency is seriously inefficient when we try to make a larger condensate. We have thought so far that the improvement of the initial conditions results in more condensed atoms even in exponential-sweep evaporative cooling. However, it is clear in Fig. 2 that a ten-fold increase of the initial number of trapped atoms does not improve the achievable number of condensed atoms. In order to obtain a larger number of condensed atoms, we have to carry out the evaporative cooling quickly at the final stage, where the system approaches the quantum degenerate region with high density, as has been demonstrated quite recently by optimizing the cooling trajectories [15, 17, 27].

B. Dependence on the initial temperature

In BEC experiments, evaporative cooling is normally employed after laser cooling [6, 30]. The atoms are transfered from a magneto-optical trap (MOT) in laser cooling into a magnetic trap in evaporative cooling. The misalignment between these two traps easily causes the fluctuations of initial temperature for succeeding evaporative cooling process. Thus, we next carried out the time-evolution calculations of evaporative cooling for several initial temperatures with the initial number of trapped atoms fixed. We assumed that 5×10^5 atoms are initially loaded into the magnetic trap before evaporative cooling (i.e., 5×10^5 atoms exist in the magnetic trap without truncation). The initial temperature was then varied from $T_i = 280$ μK to 630 μK, and we investigated how this variance of initial temperature, as well as that of the initial number of atoms, is stabilized by a three-body loss.

Figures 5(a) and 5(b) respectively show the time-evolution of the total number of atoms $\tilde{N}$ and the temperature T for several initial conditions of evaporative cooling. Both $\tilde{N}$ and T decrease almost exponentially over time. In Fig. 5(a), the small difference of $\tilde{N}$ at $t = 0$ originates from the difference of truncation-parameter value $\eta = \epsilon_t/(k_BT_i)$ for each initial temperature with the same truncation energy ϵ_t. We can see that $\tilde{N}$ curves and T curves for the initial temperatures, i.e., from 280 μK to 580 μK, finally merge into one. The variance of initial

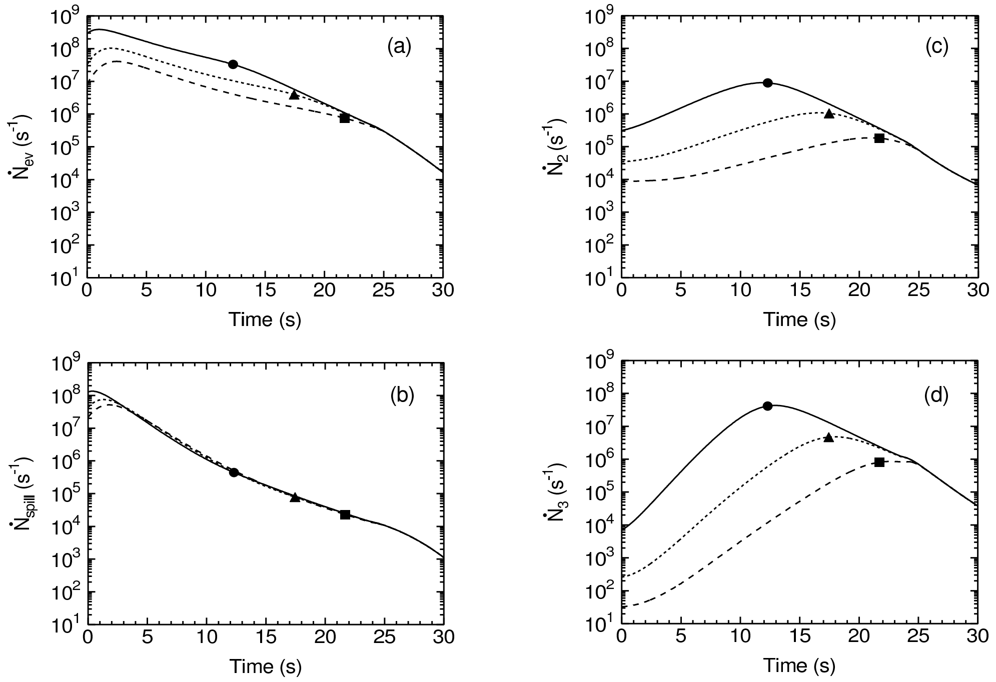

FIG. 4: Time evolution of (a) evaporation rate $\dot{N}_{\rm ev}$, (b) spill rate $\dot{N}_{\rm spill}$, (c) loss rate due to two-body dipolar relaxation $\dot{N}_2$, and (d) loss rate due to three-body recombination $\dot{N}_3$. We use the same lines as in Fig. 1 in terms of the corresponding N_i values, and show the results for the cases of $N_i = 5 \times 10^8$ (- - -), 1×10^9 (·········), and 3×10^9 (——). The symbols in the figures correspond to the same points plotted on the cooling trajectories in Fig. 3

.

temperatures finally vanishes after 30-s exponential evaporative cooling as similarly in Fig. 1.

In Fig. 6, we plot the growth of condensate at the final stage of cooling. For $T_i = 280 \sim 580$ μK, the final number of condensed atoms at $t = 30$ s takes almost the same value, $N_0 = 8.3 \times 10^4$, even though the BEC transition occurs at different times according to the initial temperatures. We will obtain the same number of condensate for a wide range of initial temperatures. When T_i exceeds 580 μK, on the other hand, the final value of N_0 decreases with increasing T_i. It is concluded that the number of condensed atoms is sufficiently stabilized against a large variance of initial temperatures too (300 μK in the present calculation). We also verified that this stabilization is caused by a combination of large three-body loss and slow evaporation at the final stage of cooling process, which is exactly the same mechanism as discussed in the previous subsection.

C. Dependence on the bias field of a magnetic trap

In BEC experiments, the magnetic trap is usually driven with a large current of the order of 100 A. The current noise causes the fluctuations and drifts of the bias field B_0 in a magnetic trap, which is the important limitation to the stable production of condensates. For example, Ref. [20] reported that the dirift of B_0 should be suppressed to less than 3 mG to obtain a good accuracy for the number of condensed atoms produced experimentally. Here we study the dependence of condensate growth on the bias field of a magnetic trap. The time-evolution calculations of 30-s evaporative cooling were carried out for several values of B_0 ranging from 1.56 to 1.614 G, under the initial conditions of $N_i = 5 \times 10^8$ and $T_i = 380$ μK. Since we used the same exponential sweeping-function of rf-field frequency $\nu_{\rm rf}(t)$, the time dependence of a truncation energy, $\epsilon_t(t)$, was equivalent in these calculations. Therefore, at any time during evaporative cooling, a larger bias field corresponds to a smaller depth of a truncated trapping potential.

Figure 7 shows the time evolution of the number of condensed atoms N_0 for the several values of bias field. The condensate growth curves strongly depend on B_0 values as has been expected. With larger bias field, the BEC transition occurs earlier and the curve shows a peak structure. A condensate gradually decays due to three-body loss since slow evaporation at the last stage of cooling can not preserve the large number of condensed atoms. On the other hand, with smaller bias field, 30-s evaporative cooling is completed before the condensate grows sufficiently. In Fig. 8, we plot the bias field dependence of the final number of condensed atoms $N_{\rm 0F}$. It is found that $N_{\rm 0F}$ is the convex function of B_0 and the stationary point exists around $B_0 = 1.585$ G. When B_0 is set at this value, we can expect that the final number of

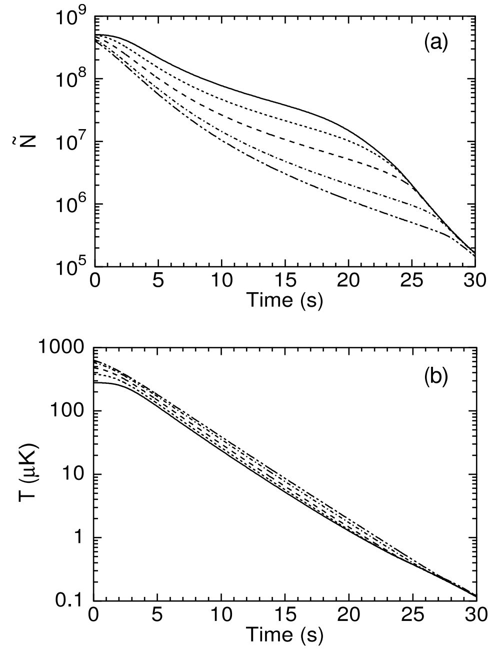

FIG. 5: Time evolution of (a) total number of atoms $\tilde{N}$ and (b) temperature T for several initial conditions of evaporative cooling: the initial temperature T_i is varied under a fixed initial number of atoms $N_i \simeq 5 \times 10^8$. In both figures, the curves correspond to the cases with $T_i = 630$ μK (—··—), 580 μK (—·—), 480 μK (- - -), 380 μK (·········), and 280 μK (——).

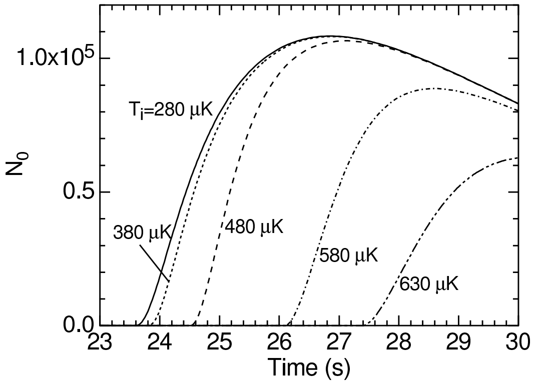

FIG. 6: Time evolution of the number of condensed atoms N_0 for several initial temperarures of evaporative cooling. We use the same lines as in Fig. 5 in terms of the corresponding T_i values.

condensed atoms is stabilized against fluctuations of bias field within about 10 mG. Note that this stabilization is also achieved by a large three-body loss.

IV. CONCLUSION

On the basis of the quantum kinetic theory of a Bose gas, we have theoretically studied the dynamics of evaporative cooling with magnetically trapped ^{87}Rb atoms. The time-evolutional calculations were carried out quantitatively for the conventional exponential-sweep cooling, which is known to be inefficient against a three-body recombination loss. We precisely examined the dependence of a condensate growth on the experimental parameters, such as the initial number of atoms, the initial temperature, and the bias field of a magnetic trap. It was shown that three-body recombination drastically depletes the trapped atoms as the system approaches the quantum degenerate region and the number of condensed atoms finally becomes insensitive to these experimental parameters. The final number of condensed atoms is well stabilized by a large nonlinear three-body loss against fluctuations of experimental conditions. We can choose the manner of evaporative cooling according to the aim of BEC experiments; a conventional exponential-sweep cooling if we want a stable production of condensates or an optimized one with the rapid sweep of rf-frequency at the final stage of cooling procedure if we want to maximize the number of condensed atoms [27].

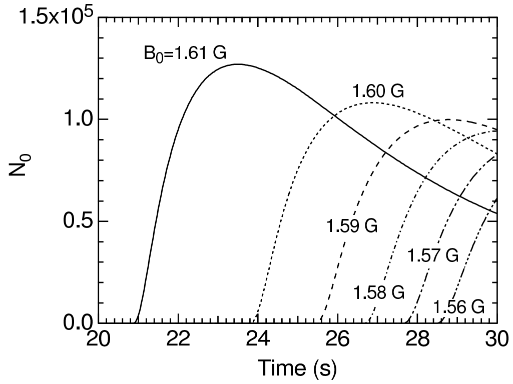

FIG. 7: Time evolution of the number of condensed atoms N_0 for several values of bias field. The curves correspond to cases with $B_0 = 1.61$ G (——) 1.60 G (·········), 1.59 G (- - -), 1.58 G (—·—), 1.57 G (—··—), and 1.56 G (—···—).

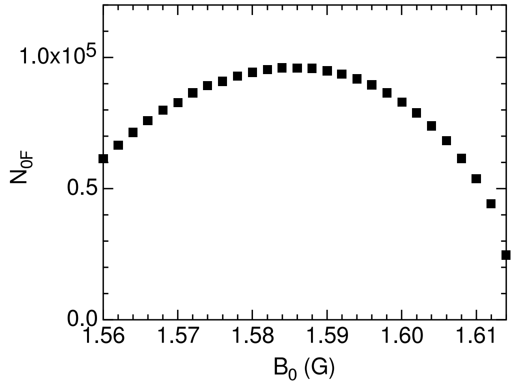

FIG. 8: Bias field dependence of the final number of condensed atoms, N_{0F}. Around the stationary point of $B_0 = 1.585$ G, we can see that N_{0F} is sufficiently stabilized against fluctuations of the B_0 value within about 10 mG .

Acknowledgments

The authors thank Y. Yoshikawa of the University of Tokyo, K. Araki, T. Kuwamoto, T. Hirano of Gakushuin University, M. Koashi, N. Imoto of the Graduate University for Advanced Studies, M. Mitsunaga of Kumamoto University, M. W. Jack of Rice University, T. Hong of the University of Washington, and Y. Tokura of NTT Basic Research Laboratories for valuable discussions.

[1] M. H. Anderson, J. R. Ensher, M. R. Matthews, C. E. Wieman, and E. A. Cornell, Science **269**, 198 (1995).

[2] C. C. Bradley, C. A. Sackett, J. J. Tollett, and R. G. Hulet, Phys. Rev. Lett. **75**, 1687 (1995); C. C. Bradley, C. A. Sackett, and R. G. Hulet, *ibid.* **78**, 985 (1997).

[3] K. B. Davis, M. -O. Mewes, M. R. Andrews, N. J. van Druten, D. S. Durfee, D. M. Kurn, and W. Ketterle, Phys. Rev. Lett. **75**, 3969 (1995).

[4] D. G. Fried, T. C. Killian, L. Willmann, D. Landhuis, S. C. Moss, D. Kleppner, and T. J. Greytak, Phys. Rev. Lett. **81**, 3811 (1998).

[5] F. Pereira Dos Santos, J. Léonard, Junmin Wang, C. J. Barrelet, F. Perales, E. Rasel, C. S. Unnikrishnan, M. Leduc, and C. Cohen-Tannoudji, Phys. Rev. Lett. **86**, 3459 (2001); A. Robert, O. Sirjean, A. Browaeys, J. Poupard, S. Nowak, D. Boiron, C. I. Westbrook, and A. Aspect, Science **292**, 461 (2001).

[6] W. Ketterle and N. J. van Druten, in *Advances in Atomic, Molecular, and Optical Physics*, edited by B. Bederson and H. Walther (Academic, New York, 1996), Vol. 37, p. 181.

[7] J. T. M. Walraven, in *Quantum dynamics of simple systems: the Forty-Fourth Scottish Universities Summer School in Physics, Stirling, August 1994*, edited by G. -L. Oppo, S. M. Barnett, E. Riis, and M. Wilkinson (IOP Institute of Physics, Bristol, 1996), Vol. 44, p. 315.

[8] R. V. E. Lovelance, C. Mehanian, T. J. Tommila, and D. M. Lee, Nature (London) **318**, 30 (1985).

[9] T. Tommila, Europhys. Lett. **2**, 789 (1986).

[10] H. F. Hess, Phys. Rev. B **34**, 3476 (1986).

[11] J. M. Doyle, J. C. Sandberg, I. A. Yu, C. L. Cesar, D. Kleppner, and T. J. Greytak, Physica B **194-196**, 13 (1994).

[12] K. B. Davis, M. -O. Mewes, and W. Ketterle, Appl. Phys. B: **60**, 155 (1995).

[13] O. J. Luiten, M. W. Reynolds, and J. T. M. Walraven, Phys. Rev. A **53**, 381 (1996).

[14] E. L. Surkov, J. T. M. Walraven, and G. V. Shlyapnikov, Phys. Rev. A **53**, 3403 (1996).

[15] C. A. Sackett, C. C. Bradley, and R. G. Hulet, Phys. Rev. A **55**, 3797 (1997).

[16] K. Berg-Sørensen, Phys. Rev. A **55**, 1281 (1997); **56**, 3308 (E) (1997).

[17] P. W. H. Pinkse, A. Mosk, M. Weideṁuller, M. W. Reynolds, T. W. Hijmans, and J. T. M. Walraven, Phys. Rev. A **57**, 4747 (1998).

[18] Yu. Kagan, B. V. Svitsunov, and G. V. Shlyapnikov, Pis'ma Zh. EkspTeor. Fiz. **42**, 169 (1985) [JETP Lett. **42**, 209 (1985)].

[19] E. A. Burt, R. W. Ghrist, C. J. Myatt, M. J. Holland, E. A. Cornell, and C. E. Wieman, Phys. Rev. Lett. **79**, 337 (1997).

[20] J. Söding, D. Guéry-Odelin, P. Desbiolles, F. Chevy, H. Inamori, and J. Dalibard, Appl. Phys. B **69**, 257 (1999).

[21] M. Holland, J. Williams, and J. Cooper, Phys. Rev. A **55**, 3670 (1997).

[22] H. Wu, E. Arimondo, and C. J. Foot, Phys. Rev. A **56**, 560 (1997).

[23] D. Jaksch, C. W. Gardiner, and P. Zoller, Phys. Rev. A **56**, 575 (1997).

[24] M. Yamashita, M. Koashi, and N. Imoto, Phys. Rev. A **59**, 2243 (1999).

[25] M. J. Holland, B. DeMarco, and D. S. Jin, Phys. Rev. A **61**, 053610 (2000).

[26] M. Yamashita, M. Koashi, Tetsuya Mukai, M. Mitsunaga, and N. Imoto, Phys. Rev. A **62**, 033602 (2000).

[27] M. Yamashita, M. Koashi, Tetsuya Mukai, M. Mitsunaga, N. Imoto, and Takaaki Mukai, Phys. Rev. A **67**, 023601 (2003).

[28] Y. Yoshikawa, K. Araki, T. Kuwamoto, and T. Hirano (private communication).

[29] F. H. Mies, C. J. Williams, P. S. Julienne, and M. Krauss, J. Res. Natl. Inst. Stand. Technol. **101**, 521 (1996); P. S. Julienne, F. H. Mies, E. Tiesinga, and C. J. Williams, Phys. Rev. Lett. **78**, 1880 (1997).

[30] H. J. Metcalf and P. van der Straten, *Laser Cooling and Trapping* (Springer-Verlag, New York, 1999).

[31] In Fig. 4(c), the time evolution of the spill rate $\dot{N}_{\mathrm{spill}}$ is almost equal for the three cases during 30-s evaporative cooling in spite of the different initial conditions. Considering that the asymptotic form of this spill rate is given by $\dot{N}_{\mathrm{spill}} \simeq 4\sqrt{2}\pi\, \dot{\epsilon}_t\, (\sqrt{m}/h)^3 \left(\int \sqrt{\epsilon_t - U(\mathbf{r})} d\mathbf{r}\right) \exp[-(\epsilon_t - \mu)/k_B T]$ and the time dependence of both ϵ_t and $\dot{\epsilon}_t$ is exactly the same for each case, the result in Fig. 4(c) implies that the value of $(\epsilon_t - \mu)/k_B T$ (i.e., the effective truncation energy for mean atom) evolves equivalently during the steady 30-s evaporative cooling.